DOI: 10.1002/chem.200903578

The *trans* Influence in the Modulation of Platinum Anticancer Agent Biology: The Effect of Nitrite Leaving Group on Aquation, Reactions with S-Nucleophiles and DNA Binding of Dinuclear and Trinuclear Compounds

Eva I. Montero,[a] Junyong Zhang,[b] Joseph J. Moniodis,[b] Susan J. Berners-Price,*[b, c] and Nicholas P. Farrell*[a, c]

Abstract: To examine the effect of leaving group and *trans* influence on the general reactivity of polynuclear platinum antitumor agents we investigated substitution of the chloride leaving groups with nitrite ion, which forms strong bonds to Pt. It was of interest to explore whether nitrite could be used to modulate biological properties of these agents, in particular the deactivating reactions that occur on reaction with S-nucleophiles, involving loss of the linking diamine under the *trans* influence of sulfur. Reported herein is a study of the synthesis, aquation, DNA binding and reactions with glutathione (GSH), methionine (Met) and acetylmethione (AcMet) of nitrito derivatives of di- and trinuclear platinum antitumor compounds: [{*trans*-$PtNO_2(NH_3)_2$}$_2$(μ-$NH_2(CH_2)_6NH_2$)]$(NO_3)_2$ (**1-NO_2**) and [{*trans*-$PtNO_2(NH_3)_2$}$_2$(μ-*trans*-$Pt(NH_3)_2${$NH_2(CH_2)_6NH_2$}$_2$)]$(NO_3)_4$ (**1′-NO_2**). {^{1}H,^{15}N}-HSQC NMR studies revealed that **1-NO_2** is inert to aquation reactions, even after prolonged incubation at physiological pH. Monitoring of the interaction of **1-NO_2** with the duplex 5′-d(ATAT**G**TACATAT)$_2$ (**I**) showed only unreacted complex, consistent with activation by aquation being a requirement for covalent DNA binding. The reaction of **1-NO_2** with GSH was studied by ^{1}H, ^{195}Pt, ^{15}N and {^{1}H,^{15}N}-HSQC NMR spectroscopy. For the parent dichlorido compounds (**1** and **1′**) substitution of chloride by GS^- leads to drug degradation involving liberation of the diamine linker. While the same final products *trans*-[$Pt(SG)_2(NH_3)_2$] (**5**) and *trans*-[{$Pt(SG)(NH_3)_2$}$_2$-μ-SG] (**6**) are formed, different mechanisms are involved, consistent with the *trans* influence $NO_2^- > Cl^-$; the half-life is slightly longer for **1-NO_2** (1.8 h) compared with **1** (1.3 h). Identification of the intermediate *trans*-[$Pt(NH_3)_2(NO_2)(SG)$] (**4**) shows that the nitrito group remains coordinated while the linker amine is substituted by coordination of GS^-, and then *trans* labilization of the nitrito group occurs leading to **5** and **6**. Reaction of the trinuclear **1′-NO_2** with GSH follows essentially the same reaction pathway. Reaction of **1-NO_2** with Met and AcMet is much slower and only 20% liberated amine was observed after reaction with Met for 24 h at 37 °C. The final product from reaction with AcMet is *trans*-[$Pt(NH_3)_2(NO_2)$-(AcMet)], as in this case coordination of the S-nucleophile does not lead to *trans* labilization of the nitrito group.

Keywords: amino acids · antitumor agents · bioinorganic chemistry · DNA · platinum

Introduction

The biological activity of platinum anticancer agents is governed by their complex chemical reactions with a variety of biomolecules.[1,2] Glutathione (GSH) and proteins and peptides containing methionine and cysteine residues, are generally considered to be responsible for the metabolic interactions of platinum drugs.[2,3] With normal intracellular concentrations of GSH ranging from 5 to 10 mM,[4] the direct coordination of GSH to platinum-containing drugs is certainly possible. These interactions are considered deactivating because the *trans* influence of sulfur has the propensity to liberate ligands coordinated *trans* to the bound sulfur.[5,6] A rel-

[a] Dr. E. I. Montero, Prof. N. P. Farrell
Department of Chemistry, Virginia Commonwealth University
Richmond, Virginia, 23284-2006 (USA)
Fax: (+1) 804-828-8599
E-mail: npfarrell@vcu.edu

[b] Dr. J. Zhang, Dr. J. J. Moniodis, Prof. S. J. Berners-Price
School of Biomedical, Biomolecular & Chemical Sciences
University of Western Australia, Crawley, WA, 6009 (Australia)

[c] Prof. S. J. Berners-Price, Prof. N. P. Farrell
Institute for Glycomics, Gold Coast Campus, Griffith University
Queensland 4222 (Australia)
Fax: (+61) 7-5552-8220
E-mail: s.berners-price@griffith.edu.au

Supporting information for this article is available on the WWW under http://dx.doi.org/10.1002/chem.200903578.

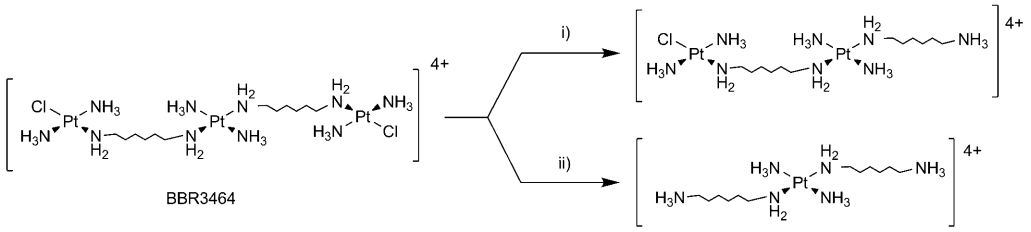

Scheme 1. Potential plasma reactions of BBR3464 under the influence of sulfur nucleophiles.

evant example is that of BBR3464, the trinuclear agent, which has undergone phase II clinical trials in humans.[7] Blood metabolism studies showed reversible and irreversible reactions with human plasma resulting in breakdown of the trinuclear structure (Scheme 1).[8] These plasma products may be mimicked by reactions of BBR3464 with S-nucleophiles especially GSH.[9] Dinuclear platinum compounds such as $[\{trans\text{-}PtCl(NH_3)_2\}_2(\mu\text{-}NH_2(CH_2)_6NH_2)](NO_3)_2$ (1,1/*t*,*t*) undergo similar reactions with loss of the linking diamine[9,10] and this reactivity appears to be general for this structure, where the Cl^- leaving group is *trans* to the linking diamine. Similar reactions may also occur in dinuclear platinum compounds linked by polyamines such as that of BBR3610, a possible "2nd-generation" analogue of BBR3464.[11]

For mononuclear compounds, a staple of platinum drug development strategies has been the use of the chelate effect in attempts to impart lesser reactivity to the molecule, for example, carboplatin contains a bidentate dicarboxylate leaving group which is more inert to substitution than the chlorides of cisplatin. This strategy is not available to di-/trinuclear compounds with $[PtN_3Cl]$ coordination spheres, that is, with monofunctional leaving groups. The carboxylate strategy has, however, been used for tetrafunctional dinuclear compounds such as $[\{Pt(mal)NH_3\}_2(H_2N\text{-}(CH_2)_6NH_2)]$.[12] To examine the effect of leaving group on the general reactivity of BBR3464 and analogs such as 1,1/*t*,*t* we investigated the use of the nitrite ion as leaving group. The nitrite group forms strong bonds to Pt and the *trans* influence and *trans* effect is $NO_2^- > Cl^-$. Few studies in platinum antitumor chemistry have used the leaving group properties of monodentate ligands less labile than chloride, in contrast to the extensive work on aqua, carboxylate and dicarboxylate ligands. Therefore it was of interest to explore whether nitrite could be used to modulate biological properties of dinuclear and trinuclear platinum agents. This paper examines the reactions of nitrite-containing platinum compounds relevant to their biological activity. Aquation and reactions with both DNA and sulfur compounds were studied. Glutathione was chosen as the principal sulfur compound for investigation because of its purported role as a determinant of cellular sensitivity to a wide variety of drugs and cytotoxic agents.

Results and Discussion

The structures of the compounds studied are shown in Figure 1. The nitrito derivatives of dinuclear (**1-NO$_2$**) and trinuclear (**1′-NO$_2$**) platinum compounds are simply prepared from the nitrate salts of the dichlorido complexes (**1** or **1′**) by treatment with 1.9 equiv of $AgNO_2$ in water, and removal of the AgCl precipitate. For ^{15}N and $\{^1H,^{15}N\}$ NMR studies fully ^{15}N-labeled **1** or **1′** were used as starting materials (synthesized as described previously).[13,14] Formation of **1′-NO$_2$** in situ, by addition of 1.99 equiv of $NaNO_2$ to a solution of **1′** in 95% H_2O/5% D_2O, was followed by $\{^1H,^{15}N\}$ HSQC NMR spectroscopy (Figure S1). The reaction proceeds via formation of the aquated intermediate (**2′**) with a half-life of about 3.5 h at 25 °C. In the absence of Ag^+ to remove the chloride ion, however, the reaction does not go to completion and an equilibrium ensues; chlorido (9%) and aqua (5%) species were still present after the addition of a further 0.3 equiv of $NaNO_2$ and prolonged incubation (Figure S1).

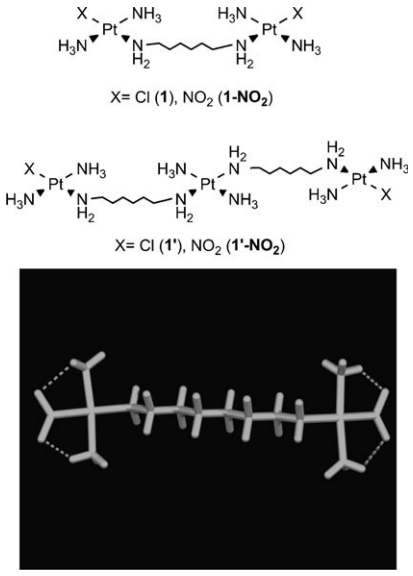

Figure 1. Structures of dinuclear and trinuclear compounds studied (top). Relativistic scalar ZORA calculated structure of **1-NO$_2$** showing hydrogen bonding between the nitrite oxygen and ammine hydrogen atoms (bottom).

The ^{15}N and ^{195}Pt NMR data for **1-NO$_2$** (Table 1) are consistent with those published before for $[Pt(NH_3)_3X]$ compounds,[15] in which the chlorido group is substituted by an *N*-bound nitrito group. The ^{195}Pt NMR signal of **1-NO$_2$** ($\delta = -2444$ ppm) shows an upfield shift ($\Delta\delta = -34$ ppm) with respect to the chlorido complex (**1**), similar in magnitude to that of the mononuclear compound. The $\{^1H,^{15}N\}$ HSQC NMR spectrum of ^{15}N-**1-NO$_2$** (Figure 2) shows two $^1H,^{15}N$ cross-peaks for the Pt–NH_3 ($\delta = 4.36/-50.8$ ppm) and Pt–NH_2 ($\delta = 4.88/-49.0$ ppm) groups. For the ammine ligand *cis* to the NO_2 group there is a strong deshielding of the ^{15}N signal ($\Delta\delta = 13.5$ ppm) with respect to the chlorido complex, whereas the ^{15}N signal of the *trans* amine group is slightly shielded ($\Delta\delta = -2.1$ ppm), similar to the trends observed for $[Pt(NH_3)_3X]$ (Table 1). There is also a strong deshielding of the ^1H signal of the *cis* NH_3 groups ($\Delta\delta = 0.47$ ppm), whereas the ^1H shift of the *trans*-NH_2 group is shielded ($\Delta\delta = -0.19$ ppm) compared to the chlorido complex. The molecular model of **1-NO$_2$** (Figure 1) shows strong hydrogen bonds between the nitrite oxygen and amine hydrogen atoms (distance = 1.87 Å), which are consistent with the deshielded ^1H and ^{15}N resonances of the NH_3 groups. These results are confirmed by the extensive hydrogen-bonding network found in *trans*-$[Pt(NH_3)_2(NO_2)_2]$.[16]

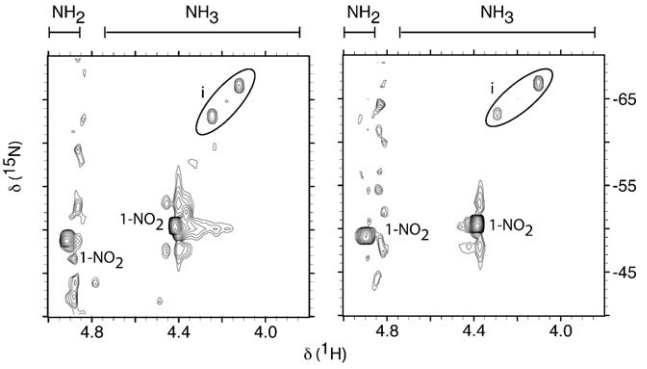

Figure 2. 2D $\{^1H,^{15}N\}$ HSQC NMR (600 MHz) spectra of **1-NO$_2$** in a) RPMI medium after incubation for 120 h at 37 °C and b) after reaction with duplex **I** (in 15 mM phosphate, pH 6.2), for 5 d. Peaks labeled "i" are due to Pt-$^{15}NH_3$ impurities in the sample of ^{15}N-**1**, as discussed previously.[13]

Table 1. Comparative ^{195}Pt and ^{15}N chemical shift for compounds with Cl and NO_2 as leaving group (X).[a]

Compound	X	δ (^{195}Pt)	Δ	δ (^{15}N) *cis* to X	Δ	δ (^{15}N) *trans* to X	Δ	Ref.
$[Pt(NH_3)_3X]^+$	Cl	−2353	−37	−66.0	13.9	−69.8	−1.1	[15]
	NO_2	−2390		−52.1		−70.9		
$[\{Pt(NH_3)X\}_2(\mu\text{-}NH_2\text{-}(CH_2)_6NH_2)]^{2+}$	Cl	−2410	−34	−64.3	13.5	−46.9	−2.1	This work
	NO_2	−2444		−50.8		−49.0		

[a] $\Delta = \delta$ (X = NO_2) − δ (X = Cl).

Aquation of 1-NO$_2$: The aquation reactions of ^{15}N-**1** and **−1′** have been previously investigated by $\{^1H,^{15}N\}$-HSQC NMR spectroscopy.[13,14,17] For **1** aquation occurs rapidly and equilibrium is achieved more rapidly ($t_{1/2} = 23$ min) than for cisplatin ($t_{1/2} = 165$ min)[18] under similar conditions (310 K). The aquation rate constant is comparable to that of cisplatin, but the chloride anation rate constant is much higher so that the equilibrium favors the dichloro form. For the trinuclear ^{15}N-**1′** the aquation rate constant is comparable to that of the dinuclear compound, but the chloride anation constant is lower so that there is a significantly greater percentage of aquated species present at equilibrium.

The aquation of ^{15}N-**1-NO$_2$** was similarly investigated here by $\{^1H,^{15}N\}$ HSQC NMR spectroscopy. For a 1 mM solution of ^{15}N-**1-NO$_2$** in 15 mM $NaClO_4$ (pH 5.8) at 25 °C, no new $^1H,^{15}N$ cross-peaks appeared after incubation for 15 days, indicating that if aquation does occur, aquated species are too low in concentration to be detected and the equilibrium strongly favors the dinitrito form. To investigate whether the nitrito derivatives could be activated under physiological conditions, a sample of ^{15}N-**1-NO$_2$** was incubated in RPMI cell culture medium (pH 7.5) at 37 °C. Again no new $^1H,^{15}N$ cross-peaks assignable to the aquated species were detected after incubation for five days (Figure 2a).

Reactions with sulfur donors (GSH): In previous work the reactions of **1** and **1′** with reduced GSH in phosphate-buffered saline, at pH 7.35, were studied by ^{195}Pt and $\{^1H,^{15}N\}$ HSQC NMR spectroscopy combined with HPLC and ESI-TOF MS.[9] Degradation of the polynuclear compounds was observed involving liberation of the diamine linker under the *trans* influence of the coordinated sulfur. The initial reaction with GSH took place rapidly (< 30 min) to form the dinuclear intermediate $[\{trans\text{-}Pt(SG)(NH_3)_2\}_2(\mu\text{-}NH_2\text{-}(CH_2)_6NH_2)]$, (**3**) and *trans* labilization of the linker occurred during a period of 7 h at 37 °C. The final products of the reaction, *trans*-$[Pt(SG)_2(NH_3)_2]$ (**5**) and the dinuclear species $[\{trans\text{-}Pt(SG)(NH_3)_2\}_2\text{-}\mu\text{-}SG]$ (**6**), were the same as formed by reaction of *trans*-$[PtCl_2(NH_3)_2]$ with GSH under the same conditions. The solution pH dictates the final product distribution of monomeric **5** (acidic pH) or dinuclear **6** (pH 7.3).

^{195}Pt NMR spectroscopy was first used to follow the reaction of **1-NO$_2$** with GSH (1:2 ratio), in 150 mM phosphate buffer pH 7.4 at 37 °C (Figure S2). The conditions are similar to those used in the previous reaction with **1**, except in that case 120 mM NaCl was used to prevent formation of aqua species and to mimic physiological conditions. No chloride was added here to avoid possible substitution reactions of the nitrito ligand, which are indicated by the equilibria observed in the reaction of **1′** with $NaNO_2$ (see above). The

initial spectrum recorded within 30 min of the start of the reaction showed three new ^{195}Pt resonances ($\delta = -2746$, -3187 and -3237 ppm), in addition to that of **1-NO$_2$** ($\delta = -2444$ ppm). The peak at $\delta = -2746$ ppm corresponds to an intermediate, as it is no longer observed after 1 h. The other two peaks correspond to the mononuclear *trans*-[Pt(SG)$_2$(NH$_3$)$_2$] (**5**, $\delta = -3237$ ppm) and bridged *trans*-[{Pt(SG)(NH$_3$)$_2$}$_2$-μ-SG] (**6**, $\delta = -3187$ ppm), as previously assigned from analysis of the *trans*-DDP reaction.[9] After 24 h the ^{195}Pt NMR spectrum (Figure S2) exhibited two peaks at $\delta = -2444$ (**1-NO$_2$**) and -3237 ppm (**5**) and 13% of the starting material remained unreacted, based on the relative integrals. Similar results were obtained in the reaction of **1-NO$_2$** with GSH in a 1:4 ratio (Figure S3), except that the final product of the reaction is the dinuclear **6**, ($\delta = -3186$ ppm) and all starting material had reacted within the first 30 min.

While these results show that the final products of the reaction of **1** and **1-NO$_2$** are the same, the intermediate species are different. For the reaction of **1**, the intermediate **3** ($\delta = -2987$ ppm), is formed by substitution of chloride by the deprotonated cysteine thiol of GSH. For **1-NO$_2$** the ^{195}Pt NMR resonance of the intermediate species appears 241 ppm downfield ($\delta = -2746$ ppm) and is assigned to *trans*-[Pt(NH$_3$)$_2$(NO$_2$)(SG)] (**4**), in which the nitrito group remains coordinated and the linker group is substituted by coordination of GS$^-$. The different mechanisms are consistent with the higher *trans* influence of the nitrito group compared with chloride, and the hydrogen bonds between the nitrite oxygen and amine hydrogen atoms (Figure 1), which will hinder substitution of the nitrito ligand. These two factors help to drive the reaction towards the formation of an intermediate where the linker is lost. Once the sulfur is bound to platinum, *trans* labilization of the nitrito group occurs leading to the same final products **5** and **6**.

To obtain further evidence for the assignment of intermediate **4** we used ^{15}N NMR to follow the reaction of **1-^{15}NO$_2$** with GSH (1:2 ratio) in 150 mM phosphate buffer (pH 7.4). Long relaxation times and lack of nuclear Overhauser effect for ^{15}N in this environment make its observation difficult, necessitating long accumulation times with concentrated samples and the reaction was followed at 20°C to slow down the kinetics. The ^{15}N NMR spectrum after 105 min is shown in Figure S4 and confirms the presence of a reaction intermediate in which the nitrito group is attached to platinum (peak **4**, $\delta = 80.0$ ppm). The two other peaks are assignable to unreacted **1-NO$_2$** ($\delta = 50.1$ ppm) and liberated NO_2^- ($\delta = 234.5$ ppm). The large coordination shifts from nitrite ion for **1-NO$_2$** ($\Delta\delta = 184$ ppm) and **4** ($\Delta\delta = 154$ ppm) are consistent with the trends observed previously for other Pt^{II}–nitrito complexes and are much larger than the coordination shifts for ammonia in Pt^{II}–ammine complexes (ca. 70 ppm). Similarly, the magnitude of the one bond ^{195}Pt,^{15}N coupling constant for **1-NO$_2$** (547 Hz) is within the range reported for other Pt^{II}–nitritito complexes and much greater than for Pt-N couplings for ammine ligands in corresponding complexes.[19]

To investigate the different reaction pathways for **1** and **1-NO$_2$** in further detail {^{1}H,^{15}N} HSQC NMR was used to follow their reactions with GSH (1: 4) in 25 mM phosphate buffer at 25°C. The pH (6.9) was lower than in the previous study, but did not change over the course of the reactions. Representative {^{1}H,^{15}N} HSQC NMR spectra from the two reactions are shown in Figure 3, the ^{1}H and ^{15}N shifts of the

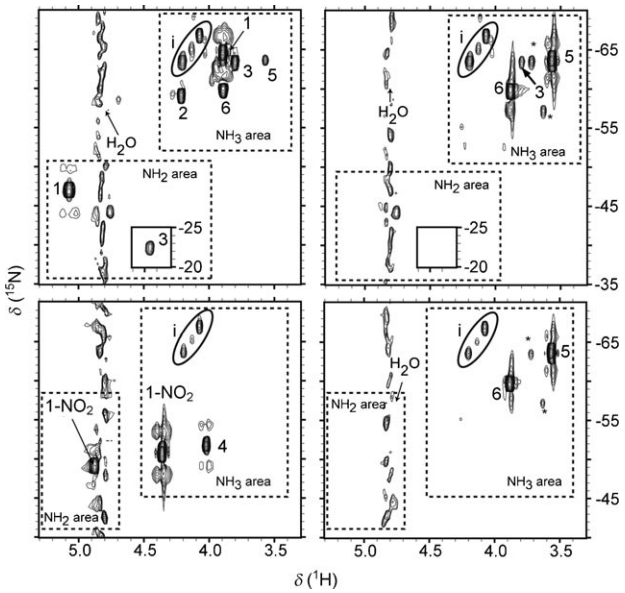

Figure 3. 2D {^{1}H,^{15}N} HSQC NMR spectra (600 MHz) spectra of 1 mM solutions of ^{15}N-**1** (top) and **1-NO$_2$** (bottom) in 25 mM phosphate buffer (pH 6.9) after reaction with GSH (4 equiv) at 25°C for (top) 1 h and 89 h and (bottom) 0.5 h and 95 h. The signals are assigned to the Pt-NH$_3$ and Pt-NH$_2$ groups of the species shown in Scheme 2. Peaks labeled "i" are due to Pt-^{15}NH$_3$ impurities in the sample of ^{15}N-**1**, as discussed previously.[13] The plots of the time dependence of the species in the two reactions are shown in Figure 4. Peaks labeled * are assigned to polymeric species.

species observed are tabulated in Table 2 and plots of their time dependence are shown in Figure 4. Representative ^{1}H NMR spectra from the same reactions are shown in Figure 5 and the different pathways for the two reactions are illustrated in Scheme 2.

Table 2. ^{1}H and ^{15}N shifts for intermediates observed during the reaction of **1**, **1-NO$_2$** and **1′-NO$_2$** with GSH (pH 6.9).

	^{15}NH$_3$[a]		^{15}NH$_2$[a]		^{15}NO$_2$[b]	
Compound	δ (^{1}H)	δ (^{15}N)	δ (^{1}H)	δ (^{15}N)	δ (^{15}N)	δ (^{195}Pt)
1	3.89	−64.3	5.07	−46.9		
2	4.21	−59.2	4.69	−58.4		
1-NO$_2$	4.36	−50.8	4.88	−49.0	50.1[c]	−2444
1′-NO$_2$[d]	4.36	−50.8	4.89	−49.0	50.1	
3	3.80	−63.5	4.45	−22.5		
4	4.02	−51.6			80.0	−2746
5	3.56	−63.6				−3237
6	3.88	−59.9				−3187

[a] ^{1}H referenced to TSP, ^{15}N referenced to ^{15}NH$_4$Cl (external), δ in ^{15}N dimension ±0.2 ppm. [b] ^{15}N referenced relative to the NO_3^- signal from 5 M ^{15}NH$_4$^{15}NO$_3$ in 2 M HNO$_3$, which is 355 ppm downfield with respect to the ^{15}NH$_4^+$ signal. [c] $^1J(^{195}\text{Pt},^{15}\text{N}) = 547$ Hz. [d] {Pt(NH$_3$)$_2$(NH$_2$R)$_2$} central linker δ ^{1}H,^{15}N = 4.20, −63.6 ppm (NH$_3$) and 4.76, −44.1 ppm (NH$_2$).

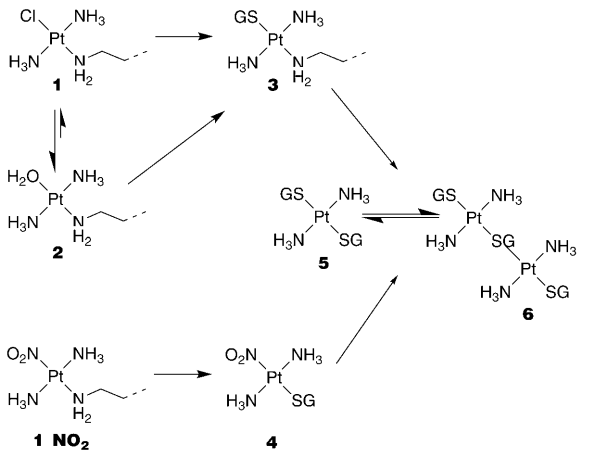

Scheme 2. Proposed reaction pathways for the reaction of **1** and **1-NO$_2$** with GSH in excess.

For the reaction of **1** with GSH (1:4), ^{1}H,^{15}N peaks for the aquated species (**2**, δ = 4.21/−59.2 ppm (NH_3), 4.69/−58.4 ppm (NH_2)) and the dinuclear intermediate (**3**, δ = 3.80/−63.5 ppm (NH_3), 4.45/−22.5 ppm (NH_2)) are visible in the first spectrum (ca. 0.5 h) along with those of unreacted **1** (δ = 3.89/−64.3 ppm (NH_3), 5.07/−46.9 ppm (NH_2)). It is likely that **3** is formed predominantly by direct reaction of **1** with GSH, as well as by rapid reaction with the aquated species (**2**), as has been reported for other reactions of Pt^{II} complexes with cysteine and GSH.[20] Once GS^- is coordinated, liberation of the *trans*-amine linker occurs rapidly, as seen in the ^{1}H NMR spectrum (Figure 5), where the characteristic triplet at δ = 3.0 ppm for the CH_2(1) protons of the released hexanediamine[9] is observed in less than 1 h and in the {^{1}H,^{15}N} HSQC NMR spectrum where a signal for the bridged *trans*-[{Pt(SG)(NH_3)$_2$}$_2$-μ-SG] (**6**, δ = 3.88/−59.9 ppm) is already just visible in the first spectrum (ca. 0.5 h). A peak for the mononuclear *trans*-[Pt(SG)$_2$(NH_3)$_2$] (**5**, δ =3.56/−63.6 ppm) is first visible after 1 h and it increases in intensity more slowly than that of the peak for **6** (Figure 4a). The intermediate **3** reaches a maximum concentration after 4.5 h and then slowly decreases until the reaction is complete (ca. 80 h). Note, however, that in the {^{1}H,^{15}N} HSQC NMR spectrum the dinuclear compound **3**, and mononuclear *trans*-[Pt(SG)(NH_3)$_2$(NH_2(CH_2)$_6$$NH_2$)]$^+$ (with dangling amine) will have identical ^{1}H,^{15}N peaks and can not be distinguished. The assignments for **5** and **6** are in accordance with those made previously,[9] and are substantiated by the time dependent changes in the Cys-βCH_2 region of the ^{1}H NMR spectrum (Figure 5). The overlapped ABM multiplets centered at δ =2.75 ppm, which increase with time, are characteristic of Cys-βCH_2 protons in a Pt-SG complex[6] and are attributable to the intermediate **3** and the final product **5**. For **6**, a characteristic strongly deshielded four line multiplet at δ =3.1 ppm represents one half of the ABM multiplet for the bridging GS environment.[6] The early appearance of this multiplet, and the relative intensity of the Cys-β-CH_2 multiplets in the final ^{1}H NMR spectrum, reflect the final product distribution (**5**>**6**) calculated on the basis of cross-peaks in the {^{1}H,^{15}N} HSQC NMR spectrum. The different product distribution observed here to that in the previous reaction at pH 7.35, where only **6** was observed, is consistent with the lower pH (**5** is favored at more acidic pH).[9]

For the reaction of **1-NO$_2$** with GSH (1:4), the first {^{1}H,^{15}N} HSQC NMR spectrum (0.5 h, Figure 3) showed ^{1}H,^{15}N peaks for unreacted **1-NO$_2$** (δ =4.36/−50.8 ppm (NH_3), 4.88/−49.0 ppm (NH_2)) and a new peak at δ =4.02/−51.6 ppm, which has no associated peak in the Pt-NH_2 region, consistent with assignment as the intermediate *trans*-[Pt(NH_3)$_2$(NO_2)(SG)] (**4**). The appearance of the triplet at δ =3.0 ppm in the ^{1}H NMR spectrum (Figure 5b) confirms that liberation of the *trans*-amine linker has begun within this timeframe and as expected (based on the aquation study) no ^{1}H,^{15}N peaks are observed for the aquated species (**2**) and hence there is no pathway to the intermediate **3**. The intermediate **4** reaches a maximum concentration after 3 h and then decreases, until it is no longer observed after 17 h. While the final product distribution (**5**>**6**) is similar to that in the reaction of **1** with GSH (under identical conditions), the time dependent plots (Figure 4) illustrate the very different reaction mechanisms involved. The bridged species **6** forms much more slowly in the reaction with **1-NO$_2$**, whereas the time dependent profile for formation of **5** is quite similar in the two reactions. Over time both reactions showed several additional minor peaks in the Pt-NH_3 region (δ ^{1}H/^{15}N 3.63 to 3.80/−57.3 to −63.6 ppm), which suggests that polymeric (GSH bridged) species could be formed, as has been observed previously for reactions of Pt^{II} complexes with GSH.[21] Whilst for both polynuclear compounds degradation involving liberation of the diamine linker is observed, these results show a slightly longer half-life for loss of the starting material in the case of **1-NO$_2$** (1.8 h) compared to **1** (1.3 h) (see Figure 4).

To confirm the generality of the observations made with **1-NO$_2$**, the reaction profile of the trinuclear **1′-NO$_2$** with GSH (1:4) was examined under the same conditions (25 mM phosphate buffer, pH 6.9, 25 °C). Representative {^{1}H,^{15}N} HSQC NMR spectra are shown in Figure 6, together with a plot showing the time dependence of the species observed. Representative ^{1}H NMR spectra from the same reaction are shown in Figure S5. It is evident from these results that **1′-NO$_2$** follows essentially the same reaction pathway as the dinuclear **1-NO$_2$**. The ^{1}H signal for liberated linker (δ =3.1 ppm) is observed within 20 min of starting the reaction and the first {^{1}H,^{15}N} HSQC NMR spectrum (ca. 25 min) shows a cross-peak at δ =4.02/−51.6 ppm, which is identical to that observed in the reaction with the dinuclear **1-NO$_2$**, further supporting its assignment as mononuclear *trans*-[Pt(NH_3)$_2$(NO_2)(SG)] (**4**) in which the amine linker is no longer coordinated. The time-dependent profile of **4** is also similar to the dinuclear case, reaching a maximum concentration after about 3 h and then decreasing until it is no longer observed after about 20 h. When the reaction is complete the {^{1}H,^{15}N} HSQC NMR spectrum (Figure 6) shows

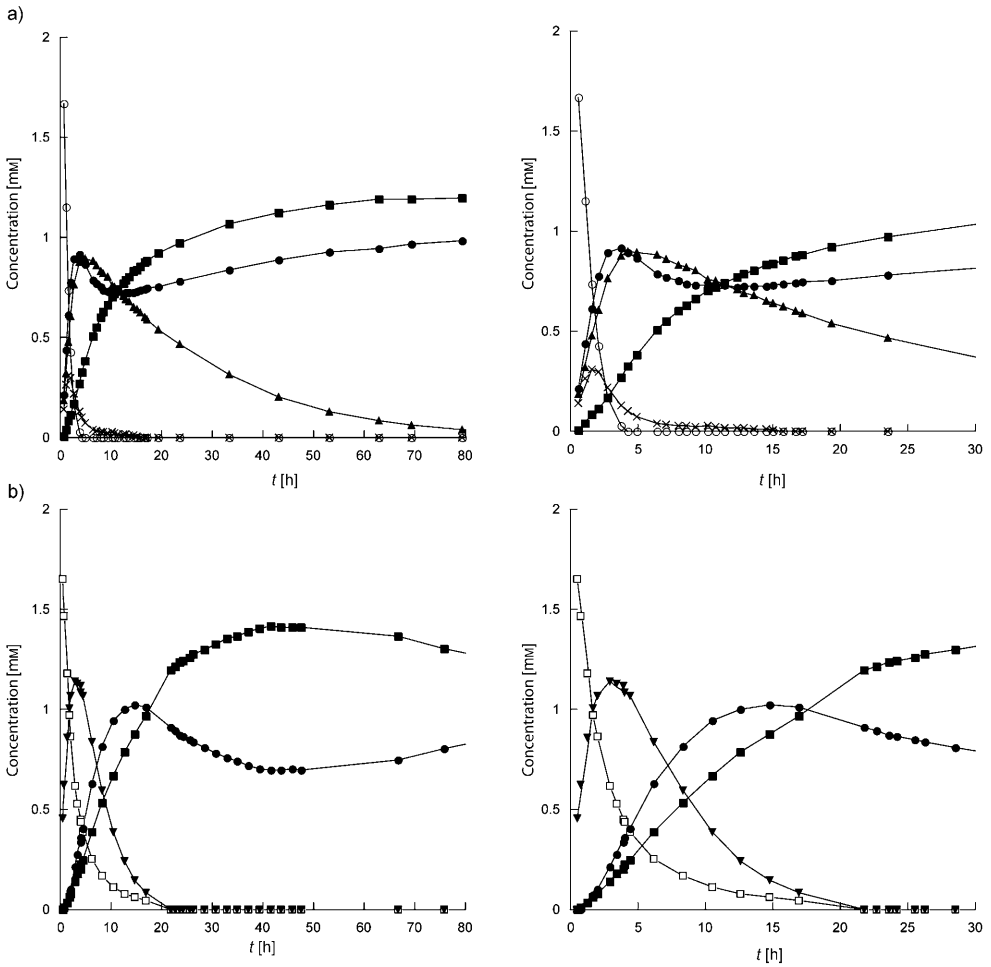

Figure 4. Plots of the relative concentrations of species observed during the reaction of a) ^{15}N-**1** and b) **1-NO$_2$** with GSH (4 equiv) in 25 mM phosphate buffer (pH 6.9) at 25 °C. The concentrations are derived from the relative volumes of the ^{1}H,^{15}N peaks in the Pt-NH$_3$ region of the {^{1}H,^{15}N} HSQC NMR spectra (Figure 3) with the dinuclear compounds treated as independent {Pt(NH$_3$)$_2$(diamine)-X} (X = Cl or NO$_2$) units. Labels: **1** (○), **1-NO$_2$** (□), **2** (x), **3** (▲), **4** (▼), **5** (■), **6** (●).

cross-peaks for the NH$_3$ (δ = 4.20/−63.6 ppm) and NH$_2$ groups (δ = 4.76/−44.1 ppm) of the liberated central {PtN$_4$} linker (which have identical ^{1}H/^{15}N shifts to those of the starting material), and the final products **5** (δ = 3.56/−63.6 ppm) and **6** (δ = 3.88/−59.9 ppm).

Reactions with sulfur donors (Met and AcMet): The reaction of **1-NO$_2$** with Met (1:2) ratio was followed by ^{1}H NMR and found to be much slower than the reaction with GSH under the same conditions. After reaction for 24 h at 37 °C only 20% liberated amine was observed, based on the appearance of the characteristic triplet at 3.0 ppm. The reactions of **1-NO$_2$** with AcMet (1:2 and 1:4) in 150 mM phosphate buffer, pH 7.5, at 37 °C were followed by ^{195}Pt (Figure S6). Again, the reaction is much slower than the GSH case with the signal for **1-NO$_2$** (δ = −2444 ppm) still present after reaction for 24 h at the higher (1:4 ratio). In both cases a new resonance appears at δ = −2789 ppm, which has similar chemical shift to that of **4** (δ = −2746 ppm) and is assigned to *trans*-[Pt(NH$_3$)$_2$(NO$_2$)(AcMet)]. This peak slowly increases in intensity, but no other ^{195}Pt NMR signals appear. The high *trans* influence of the nitrito group again leads to labilization of the *trans* amine linker, which is substituted by coordination of AcMet. In this case, however, coordination of the S-nucleophile does not lead to *trans* labilization of the nitrito group and no further substitution occurs. This is in contrast to the situation for **1**, where *trans* labilization does occur.[22]

Reaction of 1-NO$_2$ with DNA: Given these results it was of interest to examine the reactions of **1-NO$_2$** with DNA. In previous work we have investigated the stepwise formation of 1,4-GG interstrand cross-links by both ^{15}N-**1**[23] and ^{15}N-**1′**[24] on reaction with the self-complementary 12-mer duplex 5′-d(ATAT**G**TACATAT)$_2$ (**I**). The same general pathway is observed in both cases: an initial preassociation with the DNA (stronger for the more highly charged **1′**), followed by aquation, monofunctional binding and finally closure to form the bifunctional adduct. While there were differences in the rate constants for the individual steps of the reactions, the overall rate of formation of the 1,4-interstrand cross-links were similar for the di- and trinuclear complexes (com-

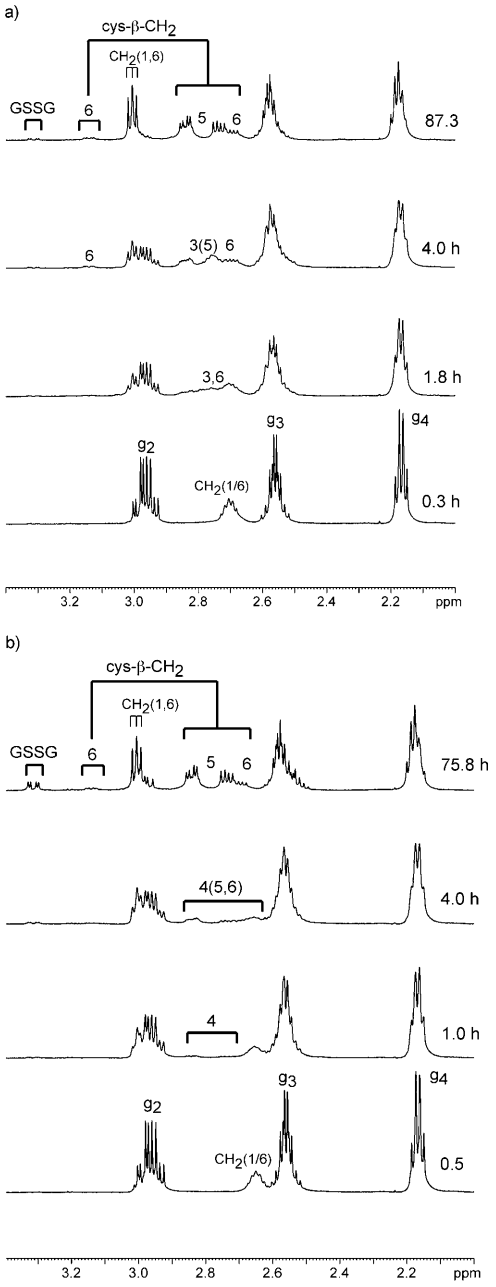

Figure 5. ^{1}H NMR spectra of reaction of a) **1** and b) **1-NO$_2$** with GSH (1:4) in 25 mM phosphate buffer (pH 6.9) at 25 °C. Drug degradation can be observed by the appearance of a triplet at 3.0 ppm for the CH_2(1) protons of the released hexanediamine.[9] This peak is observed in less than 1 h of mixing (overlapped with the cys-βCH_2 (g2) multiplet at ca. 2.9 ppm). The ABM multiplet at 2.75 ppm, which increases with time, is characteristic of cys-βCH_2 in a Pt-SG complex[6] and is attributable to the intermediates **3** and **4** and the final product **5**. The bridged glutathione species **6** has a characteristic strongly deshielded resonance at 3.1 ppm representing one half of the ABM multiplet for the bridging GSH ligand.[6]

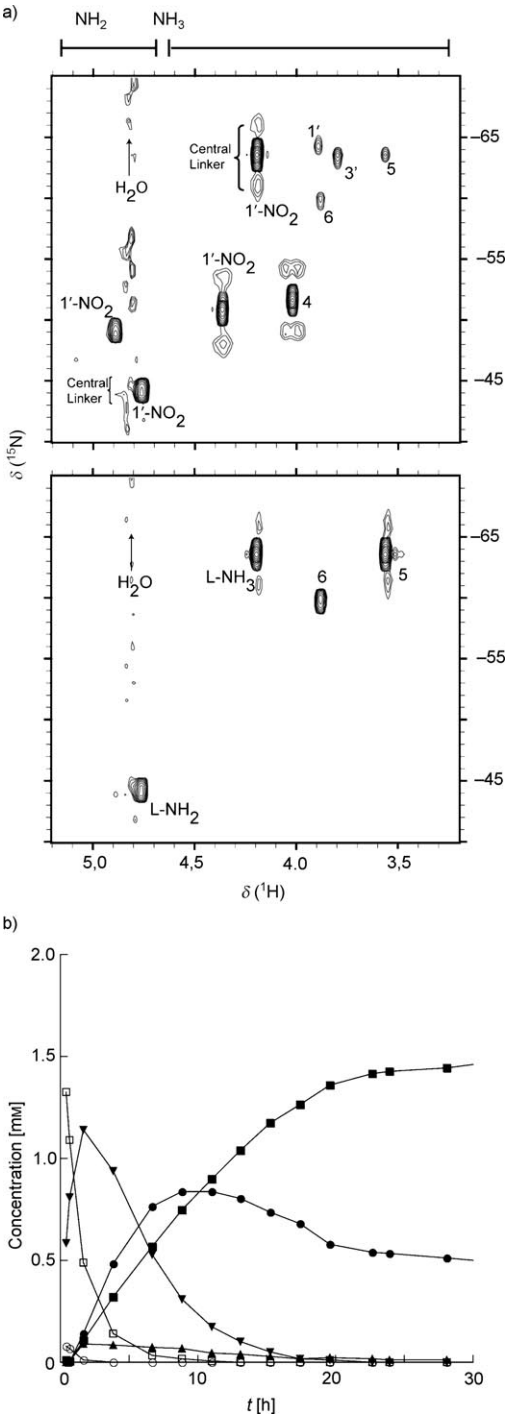

Figure 6. a) 2D {^{1}H,^{15}N} HSQC NMR spectra (600 MHz) spectra of 1 mM ^{15}N-**1′-NO$_2$** after reaction with GSH (4 equiv) at 25 °C for 1 h and 117 h in 25 mM phosphate buffer (pH 6.9). b) Plots of the relative concentrations of species observed during the reaction derived from the relative volumes of the ^{1}H,^{15}N peaks in the Pt-NH_3 region with the trinuclear species treated as independent {Pt$(NH_3)_2$(diamine)-NO_2} units. The sample of **1′-NO$_2$** contained 5 % **1′** accounting for observation of minor peaks for **3′**. Labels: **1′** (○), **1′-NO$_2$** (□), **3′** (▲), **4** (▼), **5** (■), **6** (●).

plete in ca. 50 h at 25 °C). The reaction of ^{15}N-**1-NO$_2$** with duplex **I**, was first investigated under similar conditions to these studies (15 mM phosphate buffer, 25 °C). After five days the {^{1}H,^{15}N} HSQC NMR spectrum remained unchanged showing only the two ^{1}H,^{15}N cross-peaks for the NH_3 and NH_2 groups ^{15}N-**1-NO$_2$** (Figure 2b) and no change occurred on prolonged incubation for 25 days. The reaction of ^{15}N-**1-NO$_2$** with duplex **I** was investigated also in RPMI

cell culture medium at pH 7.7 and only cross-peaks for unreacted ^{15}N-**1-NO$_2$** were observed after two days.

Overall these results indicate that **1-NO$_2$** is inert to aquation reactions, even under physiological pH conditions, and without this activation no covalent binding to the DNA occurs. ^{1}H NMR spectra recorded before and after addition of ^{15}N-**1-NO$_2$** to duplex **I** (in 15 mM phosphate buffer) do, however, provide evidence for an electrostatic interaction with the DNA. The changes in chemical shifts of the DNA protons are illustrated in Figure S7 and are consistent with minor groove binding by **1-NO$_2$**. The most significant change is for the H2 proton of A(7) ($\Delta\delta$ 0.05 ppm) and this shift is similar to that found on addition of **1′** to duplex **I**.[24] In this case the shift was attributed to binding of the charged central $\{PtN_4\}^{2+}$ linker in the minor groove as no shift changes occurred on binding of the dinuclear **1**.[23] A model for the interaction of **1-NO$_2$** and duplex **I** is shown in Figure S8, and was constructed by initially docking the complex into the minor groove, based on the observed shift changes in the ^{1}H NMR spectrum. A 10 ns molecular dynamics simulation was then performed on the system. The complex remained in the minor groove for the majority of the simulation and a representative snapshot was used for analysis (Figure S8). It can be seen from the model that the complex is deeply embedded into the minor groove. Evidence of hydrogen bonding is observed between the oxygen of the terminal NO_2 groups and H5′/H5″ protons on the DNA as well as between the terminal NH_3 groups and sugar, thymine and cytosine oxygen atoms.

Similar studies have been performed to examine the interaction of the non-covalent trinuclear platinum complex $[\{Pt(NH_3)_3\}_2(\mu\text{-}trans\text{-}Pt(NH_3)_2(H_2N(CH_2)_6NH_2)_2)]^{6+}$ (0,0,0/*t*,*t*,*t*) with duplex **I**.[25,26] In these studies, the association of 0,0,0/*t*,*t*,*t* into the minor groove did not appear to be as strong as in the case of **1-NO$_2$**, with the complex preferring a backbone tracking and groove spanning mode of binding.[26] In addition the presence of **1-NO$_2$** narrows the minor groove (when compared to free DNA), whereas the minor groove widens upon addition of 0,0,0/*t*,*t*,*t*.

Biological activity of a dinuclear nitrito compound: Early structure–activity relationship studies indicated little antitumor activity for *cis*-$[Pt(NO)_2(NH_3)_2]$.[27] To examine the biological activity of a nitrito derivative of a dinuclear compound, we modified the spermidine-linked compound $[\{trans\text{-}PtCl(NH_3)_2\}_2(\mu\text{-}H_2N(CH_2)_3NH_2(CH_2)_4NH_2)]^{3+}$, (BBR3571) which is a potential "2nd-generation" analogue of BBR3464 and exhibits remarkably similar biological properties to the trinuclear clinical agent, including DNA binding, metabolism, cytotoxicity and antitumor activity.[28–30] In growth inhibition studies, the spermidine–NO_2 compound showed significant cytotoxicity with an IC_{50} of 30 nM in HCT-116 wt colon cancer, compared with a value of <10 nM for BBR3571. The maximum tolerated dose of the spermidine–NO_2 compound is 50 mg kg^{-1} suggesting it is significantly more tolerated than its chloride counterpart (approx. 1 mg kg^{-1}).[28]

Conclusion

This contribution demonstrates a unique application of the *trans* influence in modulating biological reactions of platinum antitumor compounds. Substitution of leaving group chloride by nitrite (nitrito) reduces deactivation by glutathione, suggesting a more stable profile for nitrito derivatives with sulfur nucleophiles in general. The final products of the reaction of the nitrito compounds with GSH, bis-*trans* and S-bridged species, are analogous to those of the chloride derivatives, but slower reaction of the drug is observed, attributed to the absence of aquated intermediates. Further, the intermediate products are different to those of the chlorido compounds.

The possibility that a small percentage of nitrite compound hydrolyses to produce active aqua species, whereas metabolism reactions are dictated by the high *trans* influence of the NO_2^- group, could be reflected in a new profile of side effects. These two factors could help to improve the therapeutic index of multinuclear Pt compounds. Analogy may possibly be made with the comparison of cisplatin versus carboplatin, where in the latter case initial DNA binding and aquation is significantly less than for the more reactive Cl^- species. The cytotoxicity parameters for carboplatin also indicate a significantly less potent compound but this is overcome by the more important in vivo test where suitable activity is seen at higher doses. Given the fact that such a small percentage of administered platinum is actually considered to bind to DNA, it is possible that an analogous situation exists here.

Experimental Section

Chemicals: $NaNO_2$, $AgNO_2$, $Na^{15}NO_2$ and $^{15}NH_4{}^{15}NO_3$ (Cambridge Isotopes) were supplied by Aldrich. The sodium salt of the HPLC purified oligonucleotide 5′-d(ATAT**G**TACATAT) (**I**) was purchased from Geneworks and RPMI-1640 cell culture medium from Sigma–Aldrich. Glutathione, reduced 98% (GSH) was purchased from Acros Organics (Geel, Belgium) and was used without further purification. $Ag^{15}NO_2$ was prepared by addition of $Na^{15}NO_2$ (0.05 mg, 0.71 mmol) to a solution of $AgNO_3$ (0.123 g, 0.72 mmol) in 0.5 mL of H_2O. A light yellow compound precipitated immediately; the mixture was stirred for one hour and then the precipitate filtered off and washed with water and then dried under vacuum. Yield: 90%.

Sample preparation

$[\{trans\text{-}PtCl(^{15}NH_3)_2\}_2(\mu\text{-}^{15}NH_2(CH_2)_6{}^{15}NH_2)](NO_3)_2$ (^{15}N-1): The general synthetic pathway for the polynuclear platinum complexes has been previously described in the literature.[31] The preparation of the fully ^{15}N-labeled **1** (X = Cl) is described elsewhere.[13]

$[\{trans\text{-}PtNO_2(^{15}NH_3)_2\}_2(\mu\text{-}^{15}NH_2(CH_2)_6{}^{15}NH_2)](NO_3)_2$ (^{15}N-1-NO$_2$): ^{15}N-**1** (0.14 mmol) was dissolved in a minimum amount of H_2O to give a clear solution, then 1.98 equiv (0.27 mmol) of $AgNO_2$ were added with stirring. After stirring for 36 h at room temperature in the dark the mixture was filtered through celite and the filtrate was evaporated to dryness. The solid was dissolved in a minimum amount of H_2O, filtered and the solvent removed. The resultant solid was stirred overnight in EtOH (5 mL), then collected by filtration, washed with EtOH and dried under vacuum. Yield: 26%. ^{1}H NMR (H_2O): δ = 1.38, 1.68, 2.65, 4.34 ppm (d, ^1J(N,H) = 71.9 Hz); elemental analysis calcd (%) for $C_6H_{28}{}^{15}N_6N_4O_{10}Pt_2\cdot1.5H_2O$: C 8.74, H 3.79, N 17.73; found: C 8.78, H 3.80, N 17.36. The compound

[{*trans*-Pt^{15}NO$_2$(NH$_3$)$_2$}$_2$(μ-NH$_2$(CH$_2$)$_6$NH$_2$)](NO$_3$)$_2$ (**1-^{15}NO$_2$**) was prepared by the same method from unlabeled **1**, but using Ag^{15}NO$_2$. In the text **1** refers to the chlorido compound and **1-NO$_2$** refers to the nitrito compound, without distinction between ^{15}N labeled or unlabeled compounds. The ^{195}Pt,{^{1}H,^{15}N} HSQC and ^{15}N NMR experiments were carried out with unlabeled, ^{15}NH$_3$/^{15}NH$_2$ labeled and ^{15}NO$_2$ labeled compounds, respectively.

[{*trans*-PtNO$_2$(^{15}NH$_3$)$_2$}$_2$(μ-*trans*-Pt(^{15}NH$_3$)$_2$(^{15}NH$_2$(CH$_2$)$_6$^{15}NH$_2$)$_2$)](NO$_3$)$_4$ (^{15}N-1′-NO$_2$): The preparation of the nitrate salt of the fully ^{15}N labeled [{*trans*-PtCl(^{15}NH$_3$)$_2$}$_2$(μ-*trans*-Pt(^{15}NH$_3$)$_2$(^{15}NH$_2$(CH$_2$)$_6$^{15}NH$_2$)$_2$)]$^{4+}$ (1,0,1/*t*,*t*,*t*; ^{15}N-**1′**) is described elsewhere.[24] ^{15}N-**1′-NO$_2$** was prepared in situ by reaction of ^{15}N-**1′** (0.63 mg, 5.0×10^{-4} mmol) with 1.99 equiv of NaNO$_2$ in 95% H$_2$O/5% D$_2$O (400 μL) containing 5 μL TSP. Formation of ^{15}N-**1′-NO$_2$** at 25 °C was followed by {^{1}H,^{15}N} HSQC NMR. After 24 h the solution contained 12% **1′** and a further 0.3 equiv of NaNO$_2$ was added and reaction continued until 69 h when 9% **1′** remained (Figure S1). A solid sample of ^{15}N-**1′-NO$_2$** was prepared by reaction of ^{15}N-**1′** (0.59 mg, 4.7×10^{-4} mmol) in H$_2$O (200 μL) with 1.99 equiv of Ag^{15}NO$_2$, in an eppendorf centrifuge tube, for 19 h at room temperature. The sample was centrifuged to remove the AgCl precipitate, the supernatant filtered and the eppendorf tube rinsed with H$_2$O (100 μL). A solid was isolated after lyophilization of the solvent. Yield: 0.54 mg, 88.6%. The sample contained 5% unreacted ^{15}N-**1′** based on the relative integrals of ^{1}H,^{15}N peaks for **1′** and **1′-NO$_2$** in the {^{1}H,^{15}N} HSQC NMR spectrum.

[{*trans*-PtNO$_2$(NH$_3$)$_2$}$_2$(μ-H$_2$N(CH$_2$)$_3$NH$_2$(CH$_2$)$_4$NH$_2$)](NO$_3$)$_3$: [{*trans*-PtCl(NH$_3$)$_2$}$_2$-μ-spermidine-N^1,N^8]Cl$_3$ (0.13 mmol) was dissolved in H$_2$O (20 mL) and AgNO$_3$ (0.39 mmol, 2.97 equiv) were added with stirring. Stirring was continued for 1 h at room temperature in the dark. Then, under the same conditions, AgNO$_2$ (0.25 mmol, 1.99 equiv) was added. The mixture was stirred overnight, and then was filtered through celite. Charcoal was added to the filtrate and the suspension was stirred for 10 min at room temperature; the solid filtered off, and the filtrate was evaporated to dryness. The residue was stirred in acetone/diethyl ether 1:1 overnight. The solid was filtered off, and washed with acetone/diethyl ether 1:1. The product was recrystallized from water and subsequently from acetone/diethyl ether 1:1 and dry under vacuum. Yield: 70% ^{1}H NMR (D$_2$O): δ = 1.74 (m, 2H; H$_d$/H$_e$), 2.06 (m, 1H; H$_c$), 2.69/2.75 (m each, 2H; H$_b$/H$_b$), 3.08 ppm (m, 2H; H$_a$/H$_a$); the spermidine ligand is numbered as reported:[29] NH$_2$CH$_{2a}$CH$_{2c}$CH$_{2b}$NH$_2$CH$_{2b}$CH$_{2d}$CH$_{2e}$-CH$_{2a}$NH$_2$; ^{195}Pt NMR (D$_2$O): $\delta=-2453$ ppm. This shift is 18 ppm upfield from the analogous chloride complex; elemental analysis calcd (%) for C$_7$H$_{32}$N$_{12}$O$_{13}$Pt$_2$: C 10.12, H, 3.86, N, 20.24; found: C 10.01, H, 3.95, N, 20.55.

The biological evaluations of this compound were performed by published procedures as referenced.[29] They are not described in detail here.

Aquation experiments: ^{15}N-**1-NO$_2$** (nitrate salt) (0.32 mg, 0.4 mol) was dissolved in 400 μL of a solution of 15 mM NaClO$_4$ in 95% H$_2$O/5% D$_2$O, to give a final concentration of 1 mM. The pH of the solution was 5.8 and contained 5 μL of a 10 mM solution of 1,4-dioxane as a reference. The sample was incubated at 25 °C and {^{1}H,^{15}N} NMR spectra recorded over a period of 15 days. A second sample (final volume 480 μL) was prepared containing 1 mM ^{15}N-**1-NO$_2$** (nitrate salt) in RPMI-1640 cell culture medium containing 5% D$_2$O and 5 μL of TSP solution (sodium-3-trimethylsilyl-[D$_4$]-propionate, 13.3 mM). The pH was adjusted to 7.5 with HCl. The sample was incubated at 37 °C and {^{1}H,^{15}N} NMR spectra recorded over a period of 5 d.

DNA experiments: The HPLC purified oligonucleotide 5′-d(ATAT**G**TACATAT) was first dialyzed against 15 mM sodium acetate buffer (pH 5.4, 4 L), then freeze dried and reconstituted in deonized H$_2$O (1 mL). The concentration of the stock solution of duplex **I** (acetate concentration 225 mM) was estimated spectrophotometrically to be 3.2 mM, based on the absorption coefficient of $\varepsilon_{260}=127.5\times10^3$ M^{-1}cm^{-1}. The stock solution of **I** (124 μL) was combined with sodium phosphate buffer (211 μL, 23.9 mM, pH 5.4), D$_2$O (20 μL) and TSP solution (5 μL, 13.3 mM). The duplex was annealed by heating to 90 °C and slowly cooling to room temperature. Then a freshly prepared solution of ^{15}N-**1-NO$_2$** (40 μL, 0.32 mg, 0.4 μmol) in sodium phosphate buffer (23.9 mM, pH 5.4) was added to the duplex to reach a volume of 400 μL, with final concentrations of duplex **I** (1 mM), Na phosphate (15 mM), Na acetate (69 mM) and ^{15}N-**1-NO$_2$** (1 mM). The final pH of the solution was 6.2. The reaction was carried out at 298 K and was followed by ^{1}H and {^{1}H,^{15}N} NMR over a total time of 25 d. A second sample of duplex **I** was prepared in an identical manner, except RPMI cell culture medium (211 μL) was used instead of the phosphate buffer and ^{15}N-**1-NO$_2$** (0.36 mg, 0.45 μmol) was dissolved in RPMI medium (40 μL). The final pH of the solution was 7.7. ^{1}H and {^{1}H,^{15}N} NMR were recorded at 298 K over a period of 2 d.

Reactions with reduced glutathione (GSH): For reactions of **1-NO$_2$** monitored by ^{1}H ^{195}Pt and ^{15}N NMR a stock solution of deuterated phosphate buffer (DPB) ([phosphate] = 150 mM, pH 7.4) was prepared. The pH was measured with a Corning pH meter 340, calibrated against pH buffers of pH 4.1 and 10.1.

^{1}H NMR: **1-NO$_2$** (3.9 mg, 5×10^{-3} mmol) was dissolved in DPB (0.5 mL, 150 mM) to give a concentration of 10 mM, then 2 or 4 equiv of GSH were added.

^{195}Pt NMR: **1-NO$_2$** (10 mg, 1.3×10^{-2} mmol) was dissolved in DPB (2.5 mL, 150 mM) to give a concentration of 5.2 mM, then 2 or 4 equiv of GSH were added. Data were obtained from NMR spectra recorded at different time intervals from samples at 37 °C.

^{15}N NMR: **1-^{15}NO$_2$** (28 mg, 3.5×10^{-2} mmol) was dissolved in DPB (0.5 mL, 150 mM) to give a concentration of 14 mM, then 2 equiv of GSH were added. Data were obtained from NMR spectra recorded at different time intervals from samples at 20 °C. The solutions were maintained at the respective temperature while not in the probe. An NMR spectrum was recorded before GSH addition to each solution ($t=0$). The pH of each sample was measured at both pre- and post reaction times with values never below 7.4.

{^{1}H,^{15}N} HSQC NMR: Reactions of **1** and **1-NO$_2$** (1 mM) with GSH (4 mM) in 25 mM phosphate buffer at were carried out under identical conditions. GSH (0.61 mg, 2.0 mmol) was dissolved in a solution contained Na phosphate buffer (PB [phosphate] = 26.6 mM, pH 7.4, 400 μL), TSP (5 μL, 13.3 mM) and D$_2$O (25 μL). **1** or **1-NO$_2$** (5×10^{-3} mmol) in PB (70 μL) was added. The final pH after addition of the platinum compounds was 6.9 and did not change over time. A similar reaction of **1′-NO$_2$** (1 mM) with GSH (4 mM) in phosphate buffer (25 mM) was performed. **1′-NO$_2$** (0.54 mg, 4.2×10^{-4} mmol) was dissolved in a solution containing H$_2$O (327.5 μL), D$_2$O (21 μL) and TSP (5 μL). To this was added GSH (0.52 mg, 1.7 mmol) in Na phosphate buffer (66.5 μL, 157.9 mM, pH 7.4). The final pH was 6.9 and did not change over time. The sample of **1′-NO$_2$** contained 5% **1′**, based on the measurement of relative peak volumes in the {^{1}H,^{15}N} HSQC NMR spectra (see Figure 6a).

Reaction of 1-NO$_2$ with methionine (Met): **1-NO$_2$** (3.9 mg, 5×10^{-3} mmol) was dissolved in DPB (0.5 mL, 150 mM) to give a concentration of 10 mM. A ^{1}H NMR spectrum was recorded ($t=0$), then 2 equiv of Met were added. The temperature was maintained at 37 °C and the reaction followed by ^{1}H NMR for a period of 24 h.

Reaction of 1-NO$_2$ with acetylmethionine (AcMet): **1-NO$_2$** (10 mg, 1.3×10^{-2} mmol) was dissolved in DPB (2.5 mL) to give a concentration of 5.2 mM, then 2 or 4 equiv of AcMet were added. The temperature was maintained at 37 °C and the reaction was monitored by ^{195}Pt NMR for a period of 24 h.

NMR Spectroscopy: ^{1}H, ^{15}N and ^{195}Pt NMR one-dimensional spectra were recorded on a Varian Mercury series 300 MHz NMR spectrometer (^{1}H, 299.86 MHz; ^{15}N, 30.40 MHz; ^{195}Pt, 64.28 MHz) using a 5 mm probe for ^{1}H and ^{15}N nuclei and a 10 mm broad band probe for ^{195}Pt. ^{1}H spectra were referenced to sodium 3-(trimethylsilyl)-D$_4$-propionate (TSP). ^{15}N shifts were measured relative to the NO_3^- signal from 5 M ^{15}NH$_4$^{15}NO$_3$ in 2 M HNO$_3$, which is 355 ppm downfield with respect to the $^{15}NH_4^+$ signal. ^{195}Pt NMR spectra were referenced to the ^{195}Pt chemical shift of an aqueous solution of Na$_2$[PtCl$_4$] ($\delta=-1624$ ppm).

Two-dimensional {^{1}H,^{15}N} HSQC NMR spectra were recorded on a Bruker 600 MHz spectrometer (^{1}H, 600.13 MHz; ^{15}N, 60.81 MHz) fitted with a pulsed field gradient module and 5 mm triple resonance probehead. The ^{1}H spectra were acquired with water suppression using the watergate 3–9–19 pulse sequence[32] and the 2D {^{1}H,^{15}N} HSQC NMR spectra (optimised for $^1J(^{15}N,^1H)=72$ Hz) were recorded using standard

Bruker phase sensitive HSQC pulse sequence.[33] Samples were not spun during the acquisition of data. The samples were prepared containing 5% D_2O (sufficient for deuterium lock but with minimal loss of signal as a result of deuterium exchange in NH_3/NH_2 groups). The ^1H NMR chemical shifts were internally referenced to TSP ($\delta = 0$) and the ^{15}N chemical shifts were calibrated externally against $^{15}NH_4Cl$ (1.0 M in 1.0 M HCl in 5% D_2O/95% H_2O) at $\delta(^{15}N)$ 0.0. The ^{15}N signals were decoupled by irradiating with the GARP-1 sequence at a field strength of 6.9 kHz during the acquisition time. Typically for 1D ^1H spectra, 32/64 scans and 32 K/64 K points were acquired using a spectral width of 12 kHz and a relaxation delay of 2.5 s. For kinetics studies involving $\{^1H,^{15}N\}$ HSQC NMR spectra, 4 transients were collected for 48 or 96 increments of t_1 (allowing spectra to be recorded on a suitable timescale for the observed reaction), with an acquisition time of 0.069 s, spectral widths of 6 kHz in f_2 (^1H) and 2.1 kHz or 5.5 kHz in f_1 (^{15}N). 2D spectra were completed in 14 min and were processed using zero-filling up to the next power of 2 in both f_2 and f_1 dimension.

pH Measurements: For all $\{^1H,^{15}N\}$ HSQC NMR experiments the pH of the solutions was measured using a Shindengen ISFET (semiconductor) pH meter (pH Boy-KS723 (SU-26F)). To avoid leaching of chloride into the bulk sample, aliquots of the solution (5 μL) were placed on the electrode. The meter was calibrated using pH buffers at pH 6.9 and 4.0. Adjustments in pH were made using 0.1 M and 0.01 M H_3PO_4 or 0.1 M and 0.01 M NaOH.

Data analysis: The analyses of the reactions of **1**, **1-NO$_2$** **1′-NO$_2$** with GSH were undertaken by measuring the peak volumes in the $\{^1H,^{15}N\}$ HSQC NMR spectra using the Bruker XWINNMR software and calculating relative concentrations of $\{Pt\text{-}(^{15}NH_3)_2\}$ at each time point. For a given reaction, peak volumes were determined using an identical vertical scale and threshold value. During the reactions the dinuclear (**1**, **1-NO$_2$**) and trinuclear (**1′-NO$_2$**) compounds are broken into mono-platinum units, so the calculations are based on the initial concentration of $\{Pt(NH_3)_2\text{-}(diamine)\text{-}X\}$ (X = Cl or NO_2) units (see Figure 4).

Molecular modeling: The experimental protocol for performing density functional theory calculations and the results of these calculations have been incorporated into parameter sets which will be described in detail elsewhere.[34] The parameters for **1-NO$_2$** are supplied as Supporting Information. In this case, the results of these calculations were used to check distances of atoms for hydrogen bonding using Swiss PDB Viewer 3.7 SP5[35] and pictures were rendered in POV-Ray 3.5.[36] Molecular dynamics simulations were performed using the Amber suite of programs. Manipulations and trivial calculations were performed on a desktop PC running CENTOS Linux 5.0. All calculations involving significant CPU time were run on the Australian Partnership of Advanced Computing National Facility (APAC-NF). The DNA was equilibrated using periodic boundary conditions with a series of minimizations and molecular dynamics simulations containing gradually decreasing restraints. Subsequently, 200 ps of unrestricted dynamics was performed at 300 K with a non-bonding cut-off of 9.0 Å. Upon equilibration, the complex was docked to the proposed binding site. A constant pressure production dynamics simulation of around 10 nanoseconds at 300 K with a non-bonding cut-off of 9.0 Å was then performed on the system. Pictures were created using PDB Viewer 3.7 SP5[35] and rendered using POV-Ray 3.5.[36]

Acknowledgements

This work was supported by the Australian Research Council (Discovery grant to S.J.B.P. and N.F.), National Institutes of Health (RO1-CA78754), National Science Foundation (INT-9805552 and CHE-9615727) and the American Cancer Society (RPG89-002-11-CDD). We thank Dr. Lindsay Byrne for assistance with NMR experiments and the Australian Partnership for Advanced Computing (APAC) for access to the supercomputers.

[1] J. Reedijk, *Chem. Commun.* **1996**, 801–806; S. J. Berners-Price, L. Ronconi, P. J. Sadler, *Prog. Nucl. Magn. Reson. Spectrosc.* **2006**, *49*, 65–98; D. Gibson, *Dalton Trans.* **2009**, 10681–10689.
[2] J. Reedijk, *Chem. Rev.* **1999**, *99*, 2499–2510.
[3] A. Eastman, *Chem.-Biol. Interact.* **1987**, *61*, 241–248; Z. Guo, P. J. Sadler, *Angew. Chem.* **1999**, *111*, 1610–1630; *Angew. Chem. Int. Ed.* **1999**, *38*, 1512–1531; Y. Kasherman, S. Sturup, D. Gibson, *J. Med. Chem.* **2009**, *52*, 4319–4328.
[4] N. S. Kosower, E. M. Kosower, *Int. Rev. Cytol.* **1978**, *54*, 109–156.
[5] F. Basolo, R. G. Pearson, *Mechanisms of Inorganic Reactions*, Wiley, New York, **1967**; T. G. Appleton, J. W. Connor, J. R. Hall, P. D. Prenzler, *Inorg. Chem.* **1989**, *28*, 2030–2037; D. P. Bancroft, C. A. Lepre, S. J. Lippard, *J. Am. Chem. Soc.* **1990**, *112*, 6860–6871; D. Gibson, Y. Kasherman, D. Kowarski, I. Freikman, *J. Biol. Inorg. Chem.* **2006**, *11*, 179–188.
[6] S. J. Berners-Price, P. W. Kuchel, *J. Inorg. Biochem.* **1990**, *38*, 305–326.
[7] N. Farrell, *Met. Ions Biol. Syst.* **2004**, *42*, 251–296.
[8] V. Vacchina, L. Torti, C. Allievi, R. Lobinski, *J. Anal. At. Spectrom.* **2003**, *18*, 884–890; T. John, C. J. Ottley, D. G. Pearson, G. M. Nowell, A. H. Calvert, M. J. Tilby, *R. Soc. Chem. Spec. Publ.* **2003**, 82–90.
[9] M. E. Oehlsen, Y. Qu, N. Farrell, *Inorg. Chem.* **2003**, *42*, 5498–5506.
[10] B. A. J. Jansen, J. Brouwer, J. Reedijk, *J. Inorg. Biochem.* **2002**, *89*, 197–202.
[11] N. Summa, J. Maigut, R. Puchta, R. van Eldik, *Inorg. Chem.* **2007**, *46*, 2094–2104; J. W. Williams, Y. Qu, G. H. Bulluss, E. Alvorado, N. P. Farrell, *Inorg. Chem.* **2007**, *46*, 5820–5822; L. Zerzankova, T. Suchankova, O. Vrana, N. P. Farrell, V. Brabec, J. Kasparkova, *Biochem. Pharmacol.* **2010**, *79*, 112–121.
[12] N. Farrell, Y. Qu, J. D. Roberts in *Metallopharmaceuticals I, Vol. 1* (Eds.: M. J. Clarke, P. J. Sadler), Springer, New York, **1999**, pp. 99–115.
[13] M. S. Davies, J. W. Cox, S. J. Berners-Price, W. Barklage, Y. Qu, N. Farrell, *Inorg. Chem.* **2000**, *39*, 1710–1715.
[14] M. S. Davies, D. S. Thomas, A. Hegmans, S. J. Berners-Price, N. Farrell, *Inorg. Chem.* **2002**, *41*, 1101–1109.
[15] T. G. Appleton, J. R. Hall, S. F. Ralph, *Inorg. Chem.* **1985**, *24*, 4685–4693.
[16] J. Madarász, P. Bombicz, C. Mátyás, F. Réti, G. Kiss, G. Pokol, *Thermochim. Acta* **2009**, *490*, 51–59.
[17] J. Zhang, D. S. Thomas, M. S. Davies, S. J. Berners-Price, N. Farrell, *J. Biol. Inorg. Chem.* **2005**, *10*, 652–666.
[18] K. Hindmarsch, D. A. House, M. M. Turnbull, *Inorg. Chim. Acta* **1997**, *257*, 11–18.
[19] T. G. Appleton, K. J. Barnham, J. R. Hall, M. T. Mathieson, *Inorg. Chem.* **1991**, *30*, 2751–2756.
[20] R. N. Bose, S. Moghaddas, E. L. Weaver, E. H. Cox, *Inorg. Chem.* **1995**, *34*, 5878–5883; R. N. Bose, S. K. Ghosh, S. Moghaddas, *J. Inorg. Biochem.* **1997**, *65*, 199–205.
[21] Q. Liu, H. Wei, J. Lin, L. Zhu, Z. Guo, *J. Inorg. Biochem.* **2004**, *98*, 702–712.
[22] M. E. Oehlsen, A. Hegmans, Y. Qu, N. Farrell, *J. Biol. Inorg. Chem.* **2005**, *10*, 433–442.
[23] J. W. Cox, S. J. Berners-Price, M. S. Davies, Y. Qu, N. Farrell, *J. Am. Chem. Soc.* **2001**, *123*, 1316–1326.
[24] A. Hegmans, S. J. Berners-Price, M. S. Davies, D. S. Thomas, A. S. Humphreys, N. Farrell, *J. Am. Chem. Soc.* **2004**, *126*, 2166–2180.
[25] J. J. Moniodis, PhD thesis, The University of Western Australia (Australia), **2006**.
[26] J. J. Moniodis, Y. Qu, A. L. Harris, X. Yang, A. Hegmans, L. F. Povirk, S. J. Berners-Price, N. P. Farrell, unpublished results.
[27] M. J. Cleare, J. D. Hoeschele, *Bioinorg. Chem.* **1973**, *2*, 187–210.
[28] N. Farrell, S. Spinelli in *Uses of Inorganic Chemistry in Medicine* (Ed.: N. Farrell), RSC, Cambridge, **1999**, pp. 124–134; N. Farrell in *Platinum-Based Drugs in Cancer Therapy* (Eds.: L. R. Kelland, N. Farrell), Humana Press, Totowa, **2000**, pp. 321–338.
[29] A. Hegmans, J. Kasparkova, O. Vrana, L. R. Kelland, V. Brabec, N. P. Farrell, *J. Med. Chem.* **2008**, *51*, 2254–2260.
[30] E. I. Montero, B. T. Benedetti, J. B. Mangrum, M. J. Oehlsen, Y. Qu, N. P. Farrell, *Dalton Trans.* **2007**, 4938–4942.
[31] Y. Qu, N. Farrell, *Inorg. Chem.* **1992**, *31*, 930–932.

[32] M. Piotto, V. Saudek, V. Sklenár, *J. Biomol. NMR* **1992**, *2*, 661–665; V. Sklenár, M. Piotto, R. Leppik, V. Saudek, *J. Magn. Reson. Ser. A* **1993**, *102*, 241–245.
[33] A. G. I. Palmer, J. Cavanagh, P. E. Wright, M. Rance, *J. Magn. Reson.* **1991**, *93*, 151–170.
[34] D. S. Thomas, J. J. Moniodis, S. A. McPhee, L. A. Wedlock, A. Yusman, S. J. Berners-Price, N. P. Farrell, unpulished results.
[35] N. Guex, M. C. Peitsch, *Electrophoresis* **1997**, *18*, 2714–2723.
[36] POV-Ray rendering engine for Windows v3.5, C. Cason, http://www.povray.org/.

Received: December 30, 2009
Revised: April 19, 2010
Published online: June 29, 2010

